

# **Efficient simultaneously quantitative and qualitative detection of multiple phenols using highly water-stable**

## **Co<sup>2+</sup> - doped Cu-BTC as electrocatalyst**

Yuanfang Lia, Xiaoshu Lva, Yan Liub, Jie Yina, Ruimei Fang\*a, Guangming Jiang\*a, Zhehan Yang\*a<sup>1</sup> Chongqing Key Laboratory of Catalysis and Functional Organic Molecules, College of Environment and Resources, Chongqing Technology and Business University, Chongqing 400067, China

<sup>2</sup> Information Technology Service Center of Zhongxian Industrial Park, Chongqing 404300, PR China

### **Chemicals**

Copper(II) nitrate trihydrate (Cu(NO<sub>3</sub>)<sub>2</sub>·3H<sub>2</sub>O, 99.99%), polyvinylpyrrolidone (PVP, M<sub>w</sub>=8,000), 2-AP, 2-CP and 2-NP compounds were purchased from Aladdin (Shanghai, China). Cobalt(II) nitrate hexahydrate (Co(NO<sub>3</sub>)<sub>2</sub>·6H<sub>2</sub>O, 99%) was acquired from Adamas (Shanghai, China). Ethanol (C<sub>2</sub>H<sub>6</sub>O, 99.7%) and trimesic acid (BTC, 98%) were secured from Macklin (Shanghai, China). Sodium hydroxide (NaOH, 99.7%) was obtained from Chongqing Chuandong Chemical (Chongqing, China). All chemicals were used as received without further purification. Configuration of 0.1 M phosphate-buffered saline (PBS) is that 17.907 g Na<sub>2</sub>HPO<sub>4</sub>·12H<sub>2</sub>O, 7.8005 g NaH<sub>2</sub>PO<sub>4</sub>·2H<sub>2</sub>O, 3.7275 g KCl were dissolved in 500 mL of ultrapure water after that the resulting solution was adjusted pH and fixed volume. The 5mM [Fe(CN)<sub>6</sub>]<sup>3-/4</sup> solution is prepared as follows: 0.4116g K<sub>3</sub>[Fe(CN)<sub>6</sub>], 0.5280g K<sub>4</sub>[Fe(CN)<sub>6</sub>]·3H<sub>2</sub>O and 1.8638g KCl were dissolved in 250mL PBS solution with pH

7.0 and make up to volume in a volumetric flask.

### **Instrumentation**

X-ray diffraction (XRD) was performed using a Shimadzu XRD-6100 X-ray diffractometer (40 kV/30 mA) with Cu K $\alpha$  radiation source ( $\lambda = 1.540 \text{ \AA}$ ) at a scan rate of  $5.0^\circ \text{ min}^{-1}$  and  $2\theta$  values in the range of  $3\text{-}50^\circ$ . Field emission scanning electron microscopy (FESEM) was conducted using a Hitachi S-4800 electron microscope with an accelerating voltage of 5 kV. Transmission electron microscopy (TEM, JEOL JEM 2100) imaging was performed at an accelerating voltage of 200 kV. Fourier transform infrared (FTIR) spectra of the MOF samples were collected using a Shimadzu IRPrestige-21 spectrometer in the wavenumber region of 500 to  $4000 \text{ cm}^{-1}$ . X-ray photoelectron spectroscopy (XPS) of the sample was conducted using the Thermo escalab 250XI instrument with monochromic Al K $\alpha$  ( $h\nu=1486.6\text{eV}$ ) and at a power of 150 W. The high-resolution XPS peaks were calibrated concerning the C 1s peak at 284.8 eV and further processed using the Advantage software. Four-point probe resistivity test was conducted using the FM100GH high-precision resistivity test instrument. All the electrochemical measurements were performed at the CHI 660E electrochemical workstation. During the measurement, a standard three-electrode system including a glassy carbon working electrode (GCE,  $\phi=3 \text{ mm}$ ), platinum wire auxiliary electrode and the saturated calomel reference electrode was adopted.

### **Preparation of sodium-BTC (Na-BTC) linker**

The Na-BTC linker was prepared by adding 120 mg of NaOH and 210 mg of trimesic acid into 150 mL of ethanol. After fully dissolving, the obtained solution was heated to  $60 \text{ }^\circ\text{C}$  for 2 h in a water bath. Then, the Na-BTC product underwent centrifugation and ethanol washing three times. Finally, the product was dried at  $60 \text{ }^\circ\text{C}$  overnight.

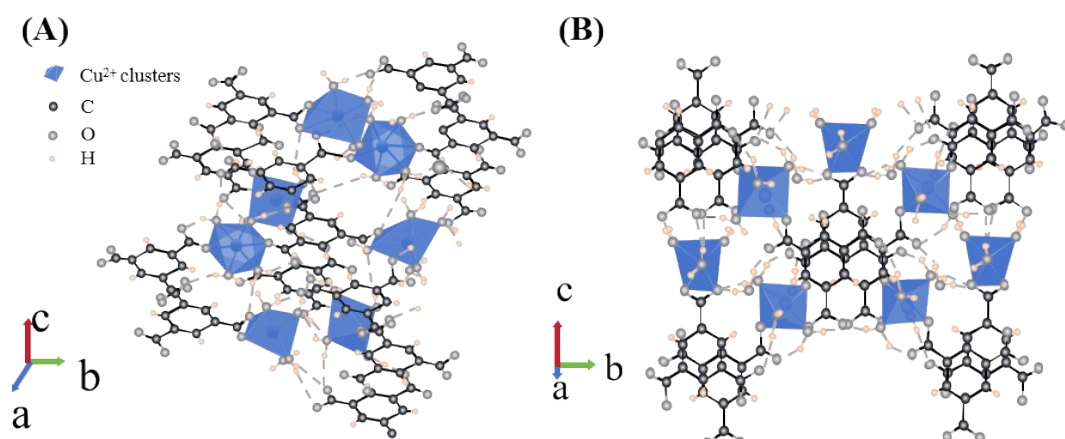


Fig. S1 (A), (B) The structure of Cu-BTC is viewed from different directions.

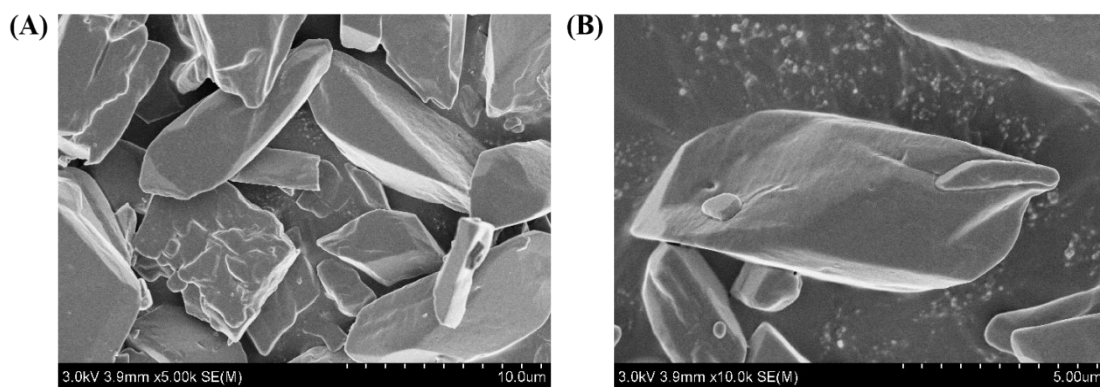


Fig. S2 (A), (B) SEM images of Cu-BTC.

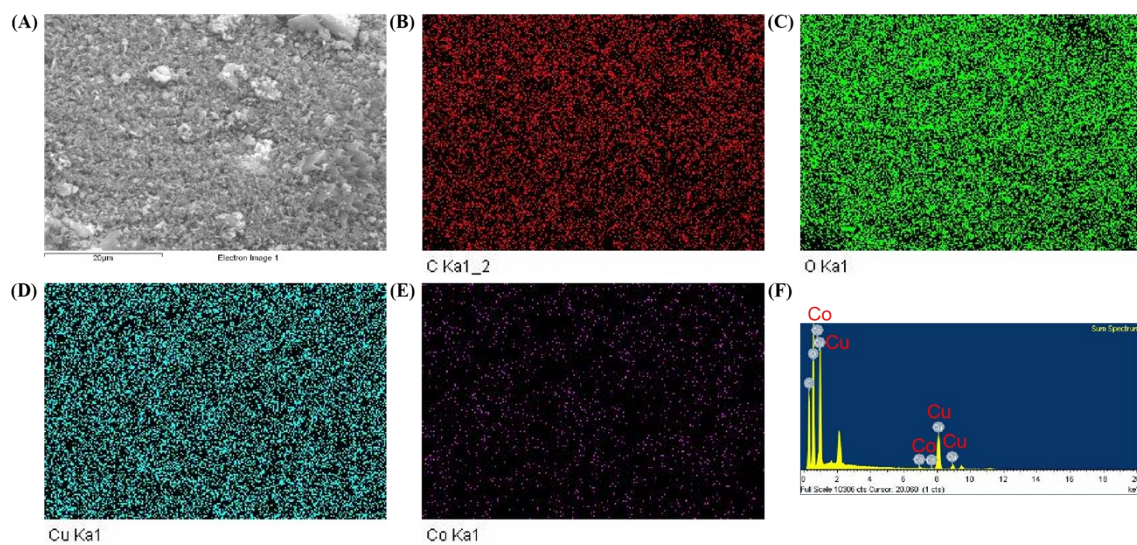


Fig. S3 (A) SEM of Cu-BTC@Co. (B)-(E) Mapping images of Cu-BTC@Co. Energy-dispersive

X-ray spectroscopy (EDS) spectrum of Cu-BTC@Co(F).

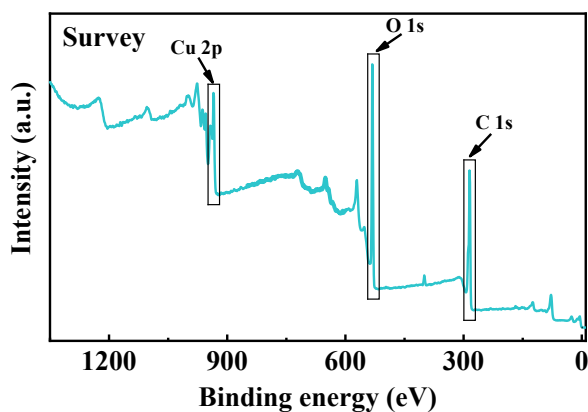


Fig. S4 The XPS survey spectra of Cu-BTC@Co.

Table S1 Relative atomic percentages of Cu, Co, O and C in Cu-BTC@Co samples based on XPS measurements.

Sample	C 1s at.%	O 1s at.%	Cu 2p at.%	Co 2p at.%
Cu-BTC@Co	60.14	30.04	6.48	0.39

Table S2 Four-point probe resistivity test results for Cu-BTC and Cu-BTC@Co.

Resistivity Test			
Materials	Pressure	Resistivity/ $\Omega \cdot m$	Conductivity (S/m)
Cu-BTC	2	1268.87	7.88E-04
	3	1209.20	8.27E-04
	4	1154.73	8.66E-04
Cu-BTC@Co	2	974.51	1.03E-03
	3	913.26	1.09E-03
	4	870.45	1.15E-03

### The electrochemical active surface area of Cu-BTC@Co/GCE

Fig. S5A illustrated the influence of scan rate on the redox behavior of Cu-BTC@Co/GCE in 2.5 mM  $[\text{Fe}(\text{CN})_6]^{3-/4-}$  solution. With the scan rate increased from 0.02 V/s to 0.1 V/s, the redox peak currents also increased with almost no shift in the redox potentials. The plot of the square root of the scan rate against the peak current for the redox process (Fig. S5B) correlation coefficient value coefficients of 0.9989 and 0.9985 for the anodic and cathodic peaks with the peak current, respectively with the regression equations of  $I_{pa} (\mu\text{A}) = 21.01911 v^{1/2} - 0.14104$  and  $I_{pc} (\mu\text{A}) = -28.18982 v^{1/2} - 1.33768$ . The electrochemical active surface area of Cu-BTC@Co/GCE is determined to be 1.457  $\text{cm}^2$  by calculating with the Randles-Sevcik equation.

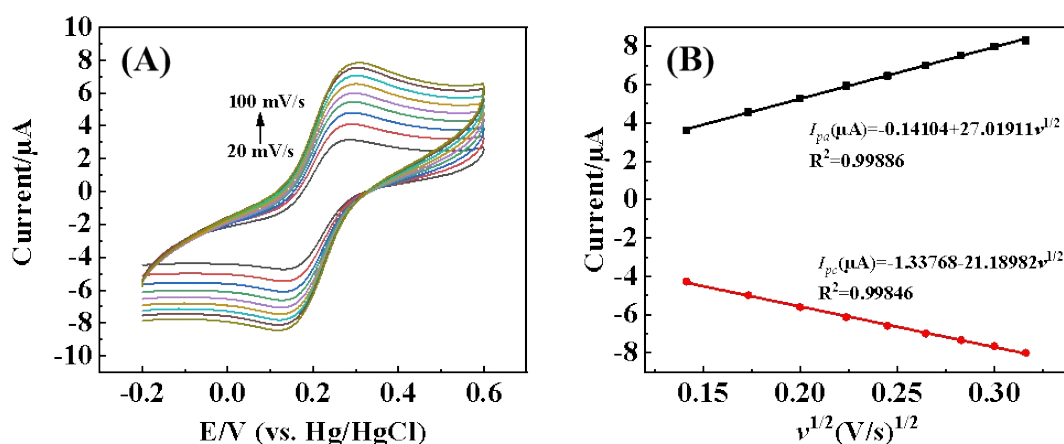


Fig. S5 (A) CVs of Cu-BTC@Co/GCE as a function of scan rate (20-100 mV/s) and the plot of the square root of scan rate vs. current (B).

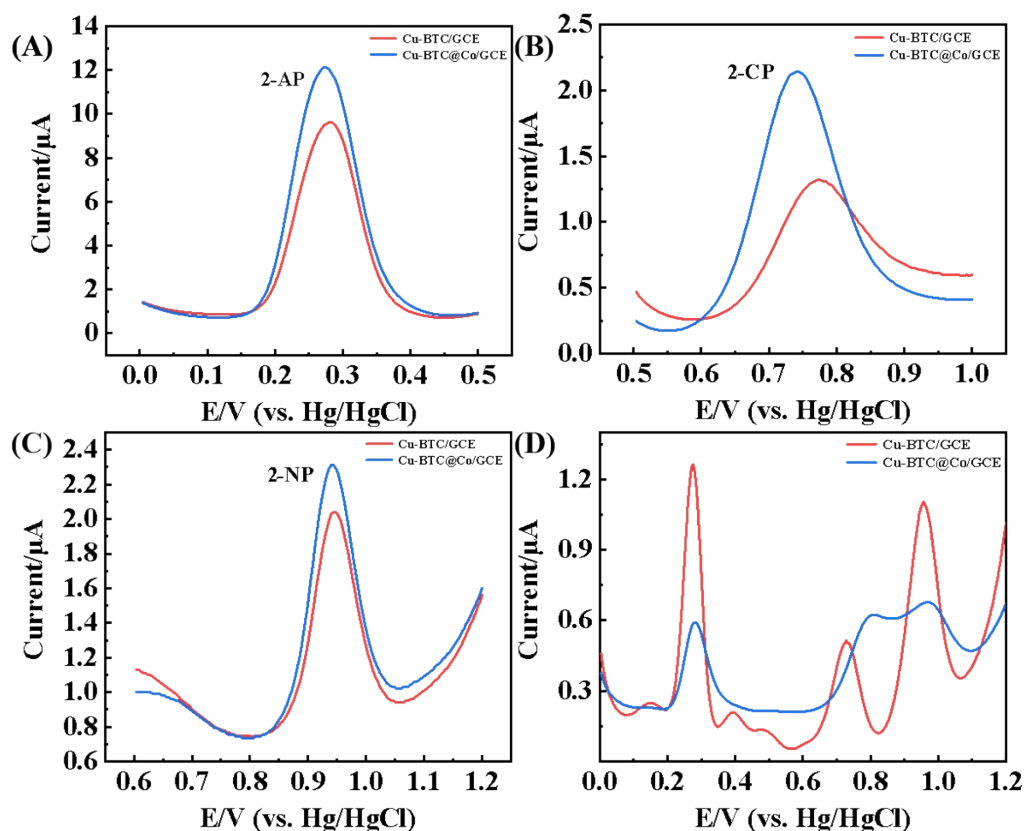


Fig. S6 (A) CV comparison graphs of Cu-BTC@Co/GCE and Cu-BTC/GCE individually detected 2-AP, 2-CP (B) and 2-NP (C). (D) DPVs were obtained for the mixture of 2-AP, 2-CP, and 2-NP in PBS (pH 5.0) at Cu-BTC and Cu-BTC@Co-modified GCE.

### Optimization of Experimental Conditions

The pH is one of the important factors affecting the electrochemical performance of electrochemical sensors. The response current of Cu-BTC@Co in 0.1 M PBS with different pH ranges (4.0 - 8.0) at the scan rate of  $0.1 \text{ Vs}^{-1}$  was tested by DPVs, and corresponding to the concentration of 2-AP, 2-CP, 2-NP was  $4.8 \mu\text{M}$ ,  $0.06 \mu\text{M}$ ,  $4.8 \mu\text{M}$ , respectively. The results are shown in Fig. S7A-C, the peak currents at pH 5 of 2-AP and 2-CP are greater than those at pH 4. However, the peak current of the target pollutants sharply declines at pH 6, due to decreased electrochemical activity of the phenols with increased alkalinity of the solution. In addition, when

comparing the response current values of 2-NP at different pH, the value at pH 5.0 showed a small difference from that at pH 6.0. In summary, considering the response currents of these three phenols at different pH values in Cu-BTC@Co/GCE, the subsequent experiment was conducted at pH 5.0.

Owing to the quantity of Cu-BTC@Co on the electrode affecting its response current values, the concentration and the volume of Cu-BTC@Co added during electrode preparation were optimized. Firstly, Cu-BTC@Co concentrations of 0.5 mg/mL, 1 mg/mL, 5 mg/mL, and 8 mg/mL were prepared. 5  $\mu$ L Cu-BTC@Co with varying concentrations was added to the bare electrode containing 12  $\mu$ M 2-AP, 0.15  $\mu$ M 2-CP and 24  $\mu$ M 2-NP. The result is shown in Fig. S7D. When the electrochemical sensor prepared was used with Cu-BTC@Co at a concentration of 1 mg/mL, the maximum oxidation peaks were observed at 2-AP, 2-CP and 2-NP. Therefore 1 mg/mL Cu-BTC@Co was the optimal concentration. To further investigate the detection performance of different volumes of 1 mg/mL Cu-BTC@Co, 2  $\mu$ L, 5  $\mu$ L and 10  $\mu$ L of 1 mg/mL Cu-BTC@Co were dropwise added onto the electrode as shown in Fig. S7E. The result showed that the sensor prepared by 5  $\mu$ L of 1 mg/mL Cu-BTC@Co exhibited excellent detection performance. To sum up, 5  $\mu$ L of 1 mg/mL Cu-BTC@Co was selected for preparing the electrochemical sensor.

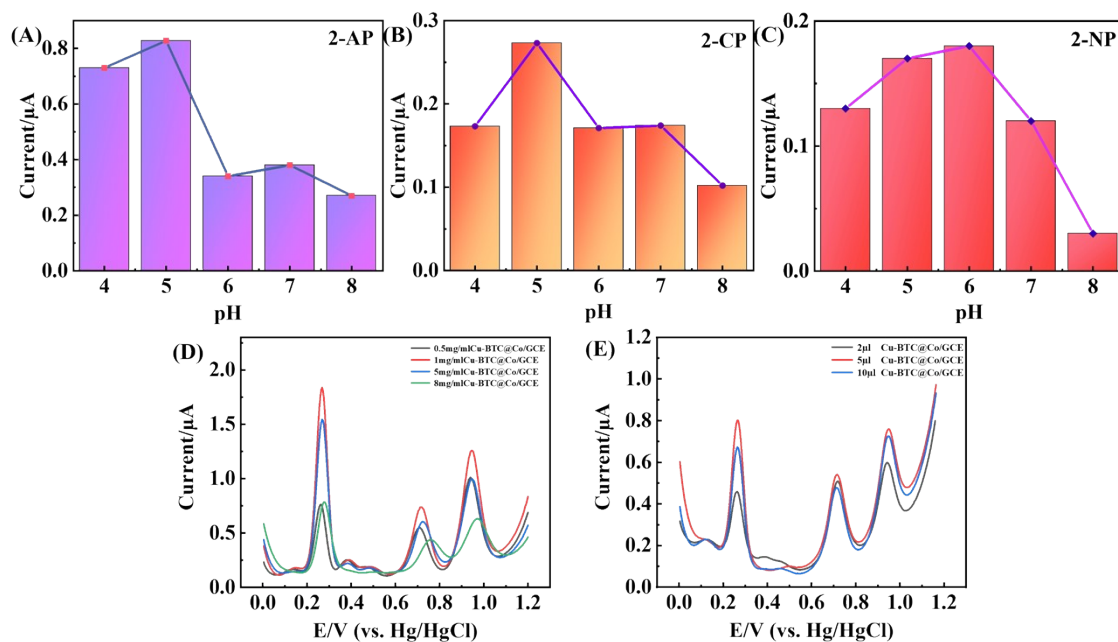


Fig. S7 (A)-(C) Peak current column-line chart of Cu-BTC@Co/GCE containing 4.8 μM 2-AP, 0.06 μM 2-CP and 4.8 μM 2-NP in 0.1 M PBS (at different pH values: 4.0, 5.0, 6.0, 7.0, 8.0). (D) DPV plots of different concentrations (0.5 mg/ml, 1 mg/ml, 5 mg/ml, 8 mg/ml) and different volumes (E) of Cu-BTC@Co for the detection of the same concentration of 2-AP, 2-CP and 2-NP.

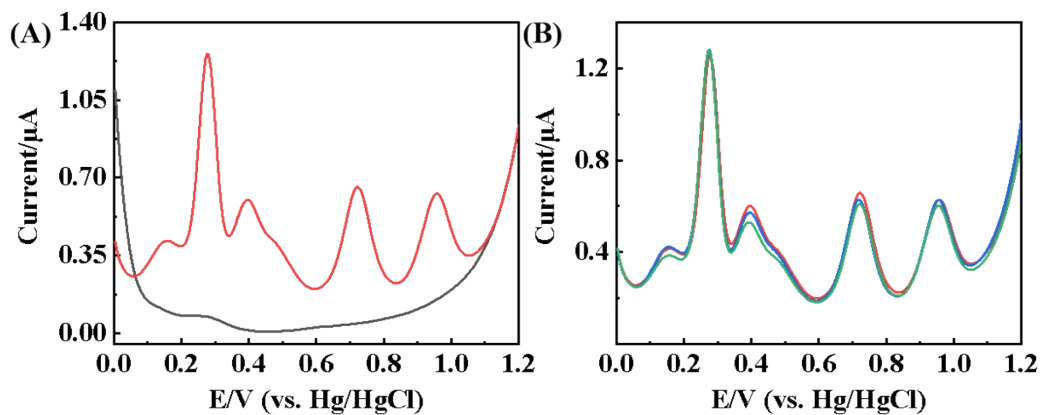


Fig. S8 (A) DPV comparison graphs of tap water and tap water addition phenols. (B) DPVs of 2-AP, 2-CP and 2-NP in tap water samples (n = 3).



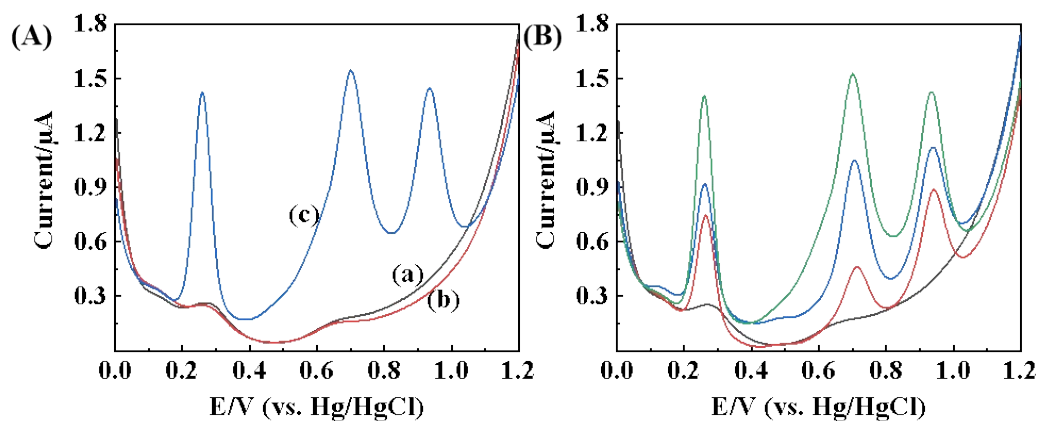
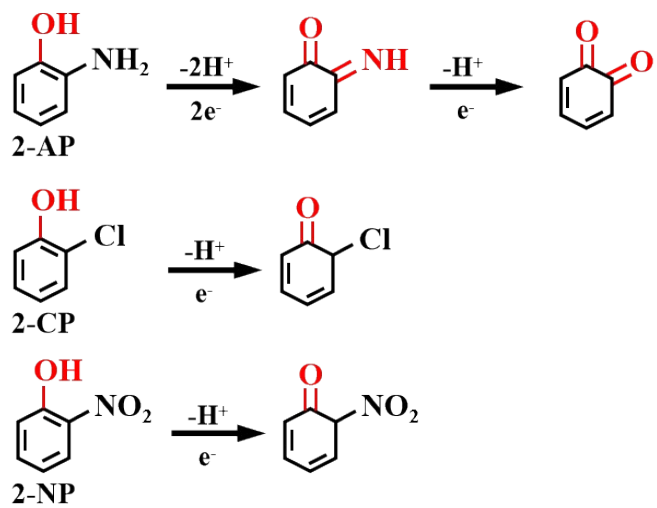


Fig. S9 (A) DPVs response of effluent samples with and without the addition of phenolic compounds. (B) DPVs of 2-AP, 2-CP and 2-NP in effluent samples.

Table S3 Recovery results of 2-AP, 2-CP and 2-NP in tap water.

sample	2-AP			2-CP			2-NP		
	Added ( $\mu\text{M}$ )	Found ( $\mu\text{M}$ )	Recovery (%)	Added ( $\mu\text{M}$ )	Found ( $\mu\text{M}$ )	Recovery (%)	Added ( $\mu\text{M}$ )	Found ( $\mu\text{M}$ )	Recovery (%)
1	9	9.05	100.5%	0.05	0.051	102%	5	5.04	100.8%
2	11	11.48	104.3%	0.09	0.088	97.8%	8	8.05	100.6%
3	15	15.35	102.3%	0.11	0.1096	99.6%	11	10.76	97.8%



Scheme 1. Mechanism of oxidation of phenolic compounds at Cu-BTC@Co/GCE